

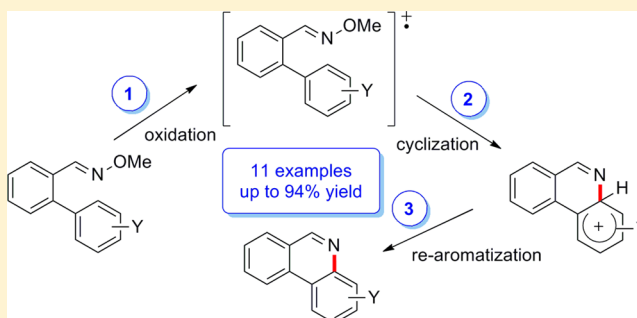
Catalytic Oxidative Cyclization of 2'-Arylbenzaldehyde Oxime Ethers under Photoinduced Electron Transfer Conditions

Julie L. Hofstra, Brittany R. Grassbaugh, Quan M. Tran, Nicholas R. Armada, and H. J. Peter de Lijser*

Department of Chemistry and Biochemistry, California State University, Fullerton, California 92834-6866, United States

S Supporting Information

ABSTRACT: A series of 2'-arylbenzaldehyde oxime ethers were synthesized and shown to generate the corresponding phenanthridines upon irradiation in the presence of 9,10-dicyanoanthracene in acetonitrile. Mechanistic studies suggest that the oxidative cyclization reaction sequence is initiated by an electron transfer step followed by nucleophilic attack of the aryl ring onto the nitrogen of the oxime ether. A concave downward Hammett plot is presumably the result of a change in charge distribution in the radical cation species with strongly electron-donating substituents that yields a less electrophilic nitrogen atom and a decreased amount of cyclized product. The reaction is selective (no nitrile byproduct is formed unlike other photochemical reactions involving aldoxime ethers) as well as regiospecific when using 2'-aryl groups with *meta*-substituents, making this reaction a useful alternative for preparing substituted phenanthridines.

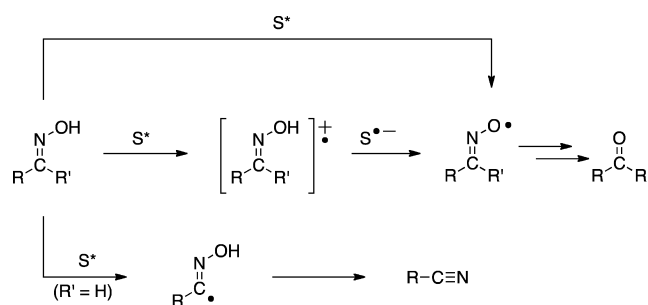


INTRODUCTION

Oximes and oxime ethers have found use in a number of applications, many of which involve reactive intermediates such as carbocations, radicals, and radical ions.^{1–3} Despite their abundance and widespread use, little is known about the reactivity of the intermediates formed in the oxidative processes of oximes and oxime ethers. Work in our lab has focused on the reactivity of oxime and oxime ether radical cations generated under photoinduced electron transfer (PET) studies. Oximes were found to react to give the parent carbonyl compounds via an electron transfer pathway when irradiated in the presence of a photosensitizer such as chloranil.^{4–6} Oximes derived from ketones reacted under these conditions to regenerate the parent ketone, whereas aldehyde oximes were found to react to give both the corresponding aldehyde and nitrile products.^{4,6} The important intermediate in the pathway that forms the parent carbonyl compound is the iminoxyl radical, which is formed via an electron transfer–proton transfer (ET–PT) sequence (for oximes with low oxidation potentials) or via a hydrogen atom transfer (HAT) pathway (for oximes with larger oxidation potentials).⁶ The nitriles were proposed to result from intermediate imidoyl radicals, which are formed via hydrogen atom abstraction at the iminyl carbon (Scheme 1).⁷

An important step in the formation of the iminoxyl radical is the deprotonation of the acidic oxime radical cation as shown by studies on a series of acetophenone⁸ and benzaldehyde oxime ethers.⁹ Studies on the PET reactions of acetophenone oxime ethers have shown that the reactivity of these substrates is solvent-dependent.⁸ In a non-nucleophilic solvent (MeCN), the product formation can be explained by a mechanism that involves electron transfer followed by proton transfer (α to the

Scheme 1. Proposed Mechanism for the Formation of Carbonyl and Nitrile Compounds from Oximes under PET Conditions^a

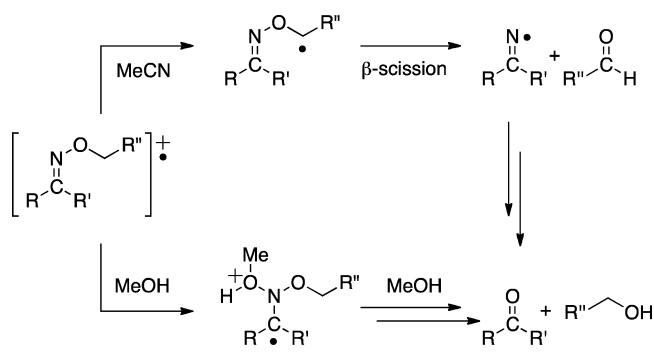


^aS* is the excited state photosensitizer.^{4–7}

oxygen) and subsequent β -scission (Scheme 2; top pathway). In a nucleophilic solvent, the mechanism is most consistent with a sequence involving electron transfer, followed by a nucleophilic attack on the nitrogen, a methanol-assisted [1,3]-proton transfer, and subsequent loss of an alcohol (Scheme 2, bottom pathway).⁸ The latter mechanism presented itself as an interesting possibility for developing a PET-induced cyclization mechanism using oxime ethers with built-in nucleophiles. For example, if aromatic rings are to act as the built-in nucleophile, attack of the aryl ring on the nitrogen of the oxime ether moiety could lead to the formation of substituted phenanthridines, providing an alternative route to the limited existing method-

Received: October 10, 2014

Published: December 1, 2014

Scheme 2. Mechanistic Pathways of Oxime Ethers upon One-Electron Oxidation^{8,9}

ologies.¹⁰ We report here our studies on the oxidative cyclization pathways of 2'-biaryl oxime ethers.

RESULTS AND DISCUSSION

Optimization of the Oxidative Cyclization Pathway.

To investigate the feasibility of the oxidative cyclization of 2'-biaryl oxime ethers, a series of reactions testing different conditions and substrates were carried out. The desired biaryl aldehydes and ketones as well as their oxime and oxime ether derivatives were prepared according to standard literature methods with minor modifications.^{11,12} Our initial photochemical experiments utilized the conditions established in previous studies.^{4–9} Most reactions were carried out on a small scale in NMR tubes using deuterated solvents in order to follow the reactions by NMR, but in addition, several reactions were carried out on a larger scale in order to isolate the product. Samples were also analyzed by gas chromatography mass spectroscopy (GC-MS) to verify product formation. As expected, irradiation of an acetonitrile or benzene solution containing the oxime and CA at 350 nm (Table 1, entries 1 and 2) resulted in the formation of the parent aldehyde and nitrile only; no cyclization was observed. Similar results were obtained with 9,10-dicyanoanthracene (DCA) as the sensitizer (entries 3 and 4), suggesting that under these conditions the pathways that lead to the parent aldehyde and nitrile products are predominant.^{4–6} In order for the oxidative cyclization to be successful, the radical cation intermediate must have a significant lifetime. Oxime radical cations are highly acidic and will deprotonate quickly,¹³ prohibiting nucleophilic attack by the aryl ring. Using the *t*-butyl oxime ether instead of the oxime with CA as the sensitizer gave promising results in acetonitrile as the solvent (entry 6). The same reaction in benzene did not give the desired product, which is presumably due to the nonpolar character of the solvent preventing electron transfer from being effective (entry 5). The oxime ethers were also found to absorb light at 300–350 nm, which led to *E/Z* isomerization of the oxime ether as well as the formation of undesirable side products, such as the parent aldehyde and nitrile. To improve the yield of the desired product, the reaction conditions were modified to use DCA as the sensitizer and 420 nm light. Under these conditions, the yield of the desired cyclic product (**2a**) increased to 43% when dissolved in acetonitrile (entry 8). The *t*-butyl ether was chosen initially because our previous work has shown that oxime ethers with hydrogen atoms present on the carbon adjacent to the oxygen can undergo deprotonation.^{8,9} However, irradiation of the oxime methyl ether gave better results than the oxime *t*-butyl ether (compare entries 8 and 9; entries 6 and 13),

Table 1. Initial Screening and Optimization of the Conditions for PET Cyclization of 2'-Biaryl Oxime Ethers

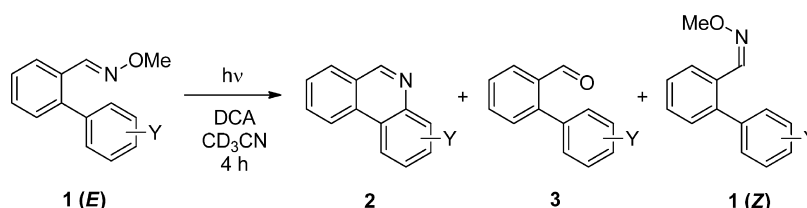
entry	R ₁	R ₂	solvent	sensor	λ (nm)	conc (mM) ^b	yield (%) ^c
1 ^d	H	H	C ₆ D ₆	CA	350	5	
2 ^d	H	H	CD ₃ CN	CA	350	5	
3 ^d	H	H	C ₆ D ₆	DCA	420	5	
4 ^d	H	H	CD ₃ CN	DCA	420	5	
5 ^d	H	<i>t</i> Bu	C ₆ D ₆	CA	350	5	
6	H	<i>t</i> Bu	CD ₃ CN	CA	350	5	19
7 ^d	H	<i>t</i> Bu	C ₆ D ₆	DCA	420	5	
8	H	<i>t</i> Bu	CD ₃ CN	DCA	420	5	43
9	H	CH ₃	CD ₃ CN	DCA	420	5	58
10 ^e	H	CH ₃	CD ₃ CN	DCA	420	5	50
11	H	CH ₃	CD ₃ CN		420		trace
12 ^e	H	CH ₃	CD ₃ CN		420		
13	H	CH ₃	CD ₃ CN	CA	420	5	28
14	H	CH ₃	CD ₃ CN	DCA	420	0.34	61
15	H	CH ₃	CD ₃ CN	DCA	420	0.17	46
16	H	CH ₃	CD ₃ CN	DCA	420	0.02	18
17 ^f	H	CH ₃	CD ₃ CN	DCA	420	5	40
18 ^f	H	CH ₃	CD ₃ CN	DCA	420	1.5	41
19 ^f	H	CH ₃	CD ₃ CN	DCA	420	0.76	49
20	CH ₃	<i>t</i> Bu	CD ₃ CN	DCA	420	5	19

^aReaction conditions unless stated otherwise: concentration of oxime ether = 15 mM; sensitizer = DCA, wavelength = 420 nm; photolysis time = 4 h; solvent = CD₃CN. ^bSensitizers have poor dissolution, thus the effective concentration is actually less than 5 mM. ^cYield was determined by ¹H NMR spectroscopy using 4-nitrobenzaldehyde and 4-nitrobenzyl bromide as internal standards. ^dReaction was run for a total of 5 h. ^eSolution was purged with Ar prior to photolysis. ^fPhotolyzed for 24 h.

suggesting that the deprotonation step is slow compared to attack by the nucleophile. Deprotonation of the oxime methyl ether leading to a high-energy primary radical may also play a role in this selectivity.

Because of this improved reactivity and because the methyl ethers are easier to prepare than the *t*-butyl ethers, all further experiments were done exclusively with the methyl derivative. The effect of dissolved oxygen on the product formation was found to be negligible (entry 10) suggesting that any radical species formed in these reactions reacts very rapidly and reaction with oxygen is not competitive. Although unusual, this is similar to previous observations from our laboratory on different systems involving the formation of highly reactive radical species.⁷ To further tune the reaction, the role of DCA was examined in more detail. As expected, in the absence of the photosensitizer, virtually no reaction occurs and none of the cyclized product is formed (entries 11 and 12). The standard reaction conditions use a catalytic amount of DCA (33 mol % photosensitizer loading); however, in these experiments, we observed that a significant amount of DCA remained undissolved throughout the reaction. Integration of the appropriate peaks in the NMR spectrum of the reaction mixture suggested that the dissolved amount of DCA was approximately 0.3 mM (2 mol %), which is significantly lower than the standard amount used in these reactions. As such, the

Table 2. Summary of Results for the PET Cyclization Reactions of 2'-Arylbenzaldehyde Oxime Ethers in Acetonitrile in the Presence of 9,10-Dicyanoanthracene



oxime ether (Y)	E^{ox} (V) ^a	ΔG_{ET}^b (kcal mol ⁻¹)	IP ^c (kcal mol ⁻¹)	yield (%) ^d		isomer ratio ^e	
				2	3	DCA	blank
H (1a)	1.79	-3.8	201.0	58	2	57:43	98:2
3-Cl (1b)	1.89	-1.6	203.0	33	3	71:29	94:6
3-OCH ₃ (1c)	1.64	-7.3	200.2	55	0	88:12	93:7
3-CH ₃ (1d)	1.78	-4.1	200.4	63	1	54:46	94:6
3-CF ₃ (1e)	1.92	-0.9	205.1	24	2	75:25	95:5
3-NO ₂ (1f)	1.93	-0.6	208.5	<2	1	70:30	64:36
4-Cl (1g)	1.88	-1.8	203.2	56	1	40:60	40:60
4-OCH ₃ (1h)	1.54	-9.6	189.1	12	1	82:18	85:15
4-CH ₃ (1i)	1.74	-5.0	200.2	94	1	59:41	88:12
4-CF ₃ (1j)	1.89	-1.5	206.2	22	5	89:11	92:8
4-NO ₂ (1k)	1.93	-0.7	209.8	trace	1	49:51	50:50
4-OPh (1l)	1.67	-6.5	191.8	59	1	66:34	93:7
3-F (1m)	1.88	-1.8	203.4	36	4	70:30	98:2

^aOxidation potentials (half-wave potentials) obtained by cyclic voltammetry. ^bCalculated free energy changes for the one-electron transfer process from the compounds to ¹DCA* in acetonitrile by the application of the Rehm–Weller equation: the excited singlet energy of DCA, 2.90 eV, and reduction potential of DCA, -0.91 V vs SCE.^{17,18} ^cCalculated (AM1) ionization potential.^{21,22} ^dAbsolute yields determined by ¹H NMR using two internal standards. ^eIsomer ratios (E/Z) determined by ¹H NMR after photolysis (most oxime ethers had an isomer ratio of >95:5 at the onset of the experiments).

amount of DCA was varied to determine the catalytic nature of the sensitizer. These experiments show that the same yield of **2a** is obtained when using a catalyst (photosensitizer) loading of 2 mol % or higher (entries 14–16). Even at 0.1 mol % DCA, a reasonable 18% yield of **2a** is obtained after 4 h of photolysis. These results suggest that the sensitizer acts as a catalyst, making this reaction attractive because of its catalytic efficiency. Although the original reaction time (4 h) was chosen arbitrarily at the onset of these experiments, studies on the time dependence of the product formation show that, in fact, this is the optimum time for the reactions using the standard amount of catalyst. The product formation reaches a maximum between 4 and 6 h of irradiation and then stabilizes. After prolonged irradiation (24 h), the product yield was found to decrease slightly (entries 17–19).

It should be noted that, in these experiments with the oxime ethers and DCA as the sensitizer, no nitrile formation is observed. Previous work in our laboratory on the PET reactions of oximes and oxime ethers derived from aldehydes typically resulted in the formation of both the parent aldehyde and the corresponding nitrile products. In many cases, the nitrile product was the major product.⁴ Existing methods for preparing phenanthridines from aldoximes or related compounds all generate significant amounts of the nitrile,^{10,14,15} and therefore, the oxidative cyclization pathway presented here is unique in that it can be used to prepare aldehyde-based phenanthridine derivatives without also producing the undesirable nitrile side products. In addition, our method is catalytic with respect to the concentration of the photosensitizer, which is a major advantage over the photosensitized cyclization method described by Walton.¹⁵ Finally, an experiment with the methyl ketone oxime ether shows that our method can also be

used to prepare ketone-based phenanthridines (entry 20), although no effort has yet been made to further optimize this reaction.

Mechanistic Studies. With the optimized conditions available, we carried out a number of experiments to investigate the mechanistic aspects of this reaction. Initial experiments involved *m*- and *p*-substituted derivatives **1a–1k**.¹⁶ The data obtained from this set of compounds indicate that, in general, both oxime ethers with electron-donating and electron-withdrawing substituents are reactive in the oxidative cyclization pathway, although oxime ethers with electron-donating substituents tended to give higher yields than those with electron-withdrawing substituents (Table 2). An obvious exception to this trend was **1h** (4-OCH₃). Using the percent yield of the substituted phenanthridines as a measure of the equilibrium constant for the reaction (K_X), analysis of this data set in a Hammett plot of the relative product formation ($\log K_X/K_H$) against σ^+ values^{19,20} gives a straight line with a slope (ρ^+) of -0.7 if the 4-OCH₃ (**1h**) derivative is excluded (Figure 1). Plotting the data against σ gave similar results, although there was more scatter in the data. To determine whether the large deviation of **1h** ($\sigma^+ = -0.778$; Figure 1) was part of a concave downward correlation, a separate experiment with the 4-OPh derivative (**1l**; $\sigma^+ = -0.50$) was carried out to corroborate this observation. Compound **1l** reacted to give the expected phenanthridine product **2l** but in lower yield than compound **1i**, confirming the downward trend.

The right-hand side of the Hammett plot (negative slope with $\rho^+ = -0.7$) clearly suggests the involvement of a species with a developing positive charge, which is consistent with a pathway involving reactive intermediates generated by an oxidative PET process.^{5,6} Previously, the photochemical

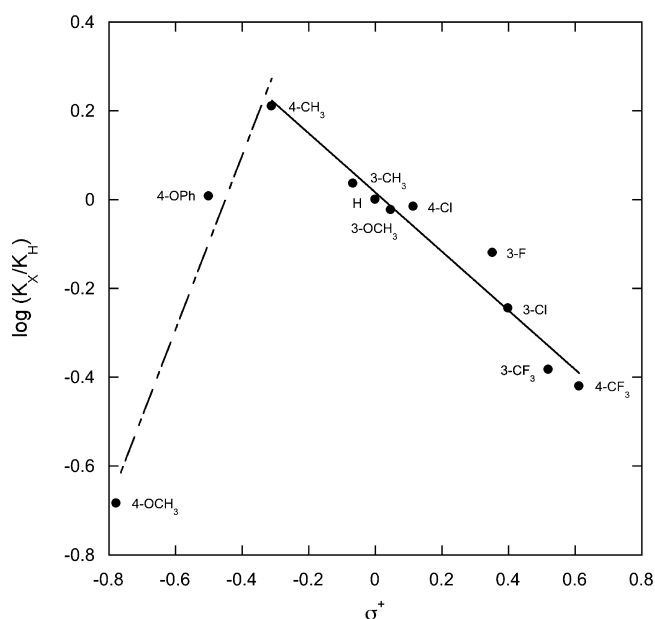


Figure 1. Hammett plot of PET cyclization reaction of substituted 2'-arylbenzaldehyde oxime ethers.

reactions of oxime esters studied by Rodriguez¹⁴ and Walton¹⁶ were proposed to proceed via iminyl radical intermediates. A plot of the data points from Walton's study against σ^+ shows a line with a slope that is close to zero, consistent with a neutral radical intermediate such as the iminyl radical.¹⁵ Deb and Yoshikai¹⁰ studied a transition-metal-catalyzed cyclization reaction of *O*-acetyl oximes and proposed a Friedel–Crafts-type mechanism. The slope of the data points is in agreement with the formation of an intermediate with a developing positive charge. However, comparing the data sets (Figure 2), it is obvious that in our system a different mechanism operates.

Further support for an electron transfer mechanism comes from electrochemical and computational data. The measured

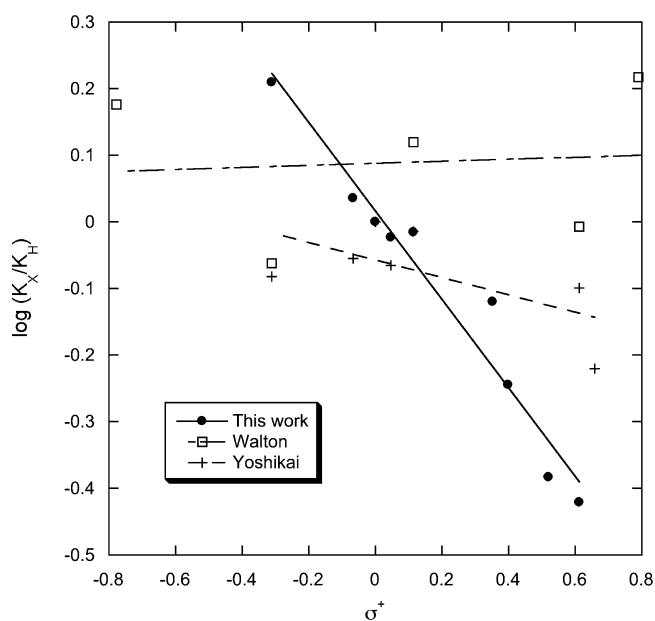


Figure 2. Hammett plots of data from our study compared to data from previous studies.^{10,15}

oxidation potentials for the oxime ethers indicate that the free energy of electron transfer (ΔG_{ET}) is negative in all cases, which makes the PET pathway favorable, although none of the reactions are expected to be diffusion-controlled (Table 2).¹⁷ Plotting the peak potentials (E_p) of the oxime ethers against σ^+ gives a reasonable correlation (Figure 3), although there is

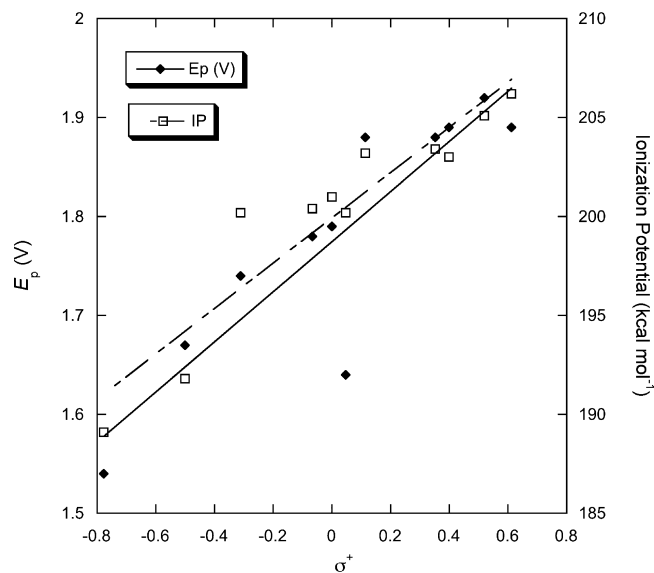


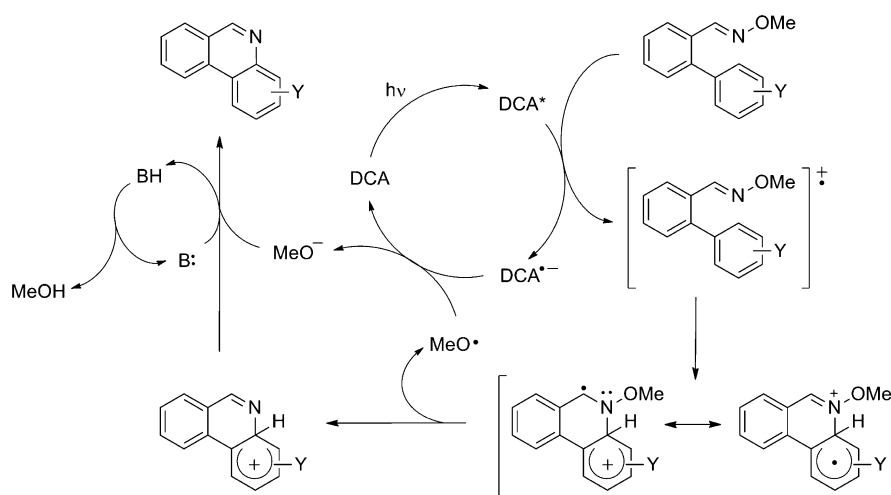
Figure 3. Correlation of measured peak potentials (E_p) and calculated ionization potentials (IP) with σ^+ for a series of substituted 2'-arylbenzaldehyde *O*-methyl oxime ethers.

more scatter as compared to the data plotted in Figure 1. Previously, we have used calculated ionization potentials (IP) as an alternative method for correlating the reactivity of substituted oximes in PET reactions.^{5,6} Plotting the calculated ionization potentials (AM1, kcal/mol)^{21,22} against σ^+ also shows a reasonable correlation (Figure 3), supporting the electron transfer mechanism.

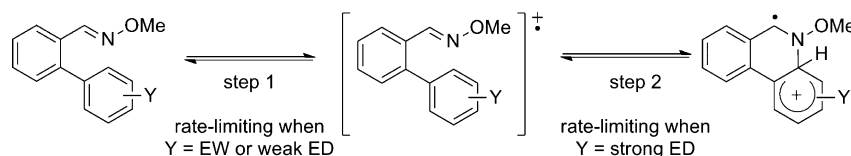
On the basis of these results, we propose a mechanism for the conversion of 2'-arylbenzaldehyde oxime ethers to the corresponding phenanthridines in which the initial step involves oxidation of the oxime ether to the corresponding radical cation intermediate (Scheme 3). Nucleophilic attack by the aromatic ring onto the nitrogen of the oxime ether radical cation leads to the formation of a resonance-stabilized distonic radical cation, which can be represented as a structure containing a Wheland-type cation and an α -amino radical. Work by Gould and co-workers has shown that these types of α -amino radicals undergo very rapid N–O bond homolysis.²³ This reaction would produce a cyclized cation and a methoxy radical, which is reduced by the DCA radical anion to regenerate the photosensitizer. The methoxy anion is converted to methanol by abstraction of a proton from the cyclized cation intermediate, which generates the final phenanthridine product. This proposed mechanism is consistent with the catalytic role of DCA as it is regenerated in the reaction. Furthermore, NMR spectra of the crude product mixtures clearly show the formation of methanol as a product in the reaction.

The Hammett data (Figure 1) show a concave downward trend for the oxime ethers with strong electron-donating substituents (1h, 1l). This type of trend has traditionally been associated with mechanistic pathways where there is a change in the rate-determining step.²⁰ This explanation is consistent with

Scheme 3. Proposed Mechanism for the Formation of Phenanthridines from the 2'-Arylbenzaldehyde O-Methyl Oxime Ether Radical Cation Intermediate



Scheme 4. Change in Rate-Limiting Step as a Function of Substituent in the PET Reactions of 2'-Arylbenzaldehyde O-Methyl Oxime Ethers



our proposed mechanism (Scheme 3). Assuming that N–O homolysis (loss of the methoxy radical) and loss of the proton in the last (re-aromatization) step are both fast, we can simplify the mechanism as shown in Scheme 4. Step 1 is the rate-limiting step for compounds appearing on the right side of Figure 1 ($\sigma^+ > -0.3$), whereas step 2 is rate-limiting for compounds with strong electron-donating substituents on the left side of Figure 1 ($\sigma^+ < -0.3$). For the oxime ethers with electron-withdrawing and weakly electron-donating substituents, step 1 (electron transfer) is rate-limiting. Electron transfer is much less favorable for compounds with electron-withdrawing substituents (as seen by the higher E_p and IP values) and raises the energy of the radical cation intermediate. The high-energy intermediate then reacts rapidly via an internal nucleophilic attack by the aromatic ring on the nitrogen atom of the oxime ether. When the substituents are strongly electron-donating (4-OCH₃ and 4-OPh), significantly lower oxidation and ionization potentials are observed and step 1 becomes more favorable. Additionally, these substituents stabilize the radical ion intermediate, making nucleophilic attack by the aromatic ring (cyclization) less favorable, and as a result, step 2 becomes rate-limiting.

An alternative explanation would be that the decreased reactivity is a result of changes in the charge distributions in the radical cation as a function of the substituents. For the oxidative cyclization reaction to occur, a significant positive charge development is expected on the nitrogen atom. Therefore, if the charge development on the nitrogen decreases as a result of substituent effects elsewhere in the molecule, the aryl ring is less likely to attack the nitrogen and form the cyclized product. To investigate this possibility, we focused on the calculated (AM1) charge densities in the neutral and radical cation species of oxime ethers **1h** and **1i**. The AM1 program calculates atomic electrostatic charges (ESP) and natural atomic charges; both

were used for this analysis and were found to give similar results. The data presented and discussed here are an average of the differences in charge distribution between the neutral and the radical cation as calculated by the two methods. A summary of these data is listed in Table 3; the complete data set can be found in the Supporting Information. For compound **1i**, it can

Table 3. Summary of Calculated (AM1) Changes in Atomic Charge Distributions for Non-Hydrogen Atoms between the Neutral and Radical Cation Structures of Oxime Ethers **1h** and **1i** (Atom Labels Refer to Figure 4)

	oxime ether 1h			oxime ether 1i		
	% Δ^a	% Δ^b	avg	% Δ^a	% Δ^b	avg
C1	1%	1%	1%	3%	2%	2%
C4	3%	2%	3%	−4%	−2%	−3%
C2	5%	2%	3%	14%	13%	14%
C6	7%	4%	5%	5%	4%	4%
C5	1%	2%	1%	20%	14%	17%
C3	−17%	−10%	−14%	17%	11%	14%
C7	0%	1%	1%	4%	1%	3%
N1	−5%	−6%	−5%	9%	11%	10%
O1	3%	3%	3%	9%	8%	9%
C8	0%	−1%	−1%	−1%	−3%	−2%
C9	23%	20%	22%	−13%	−9%	−11%
C10	20%	12%	16%	5%	4%	4%
C11	2%	−1%	0%	2%	1%	1%
C12	9%	4%	7%	2%	1%	1%
C13	0%	3%	1%	2%	1%	1%
C14	7%	7%	7%	2%	1%	1%
O2	10%	13%	12%			
C15	2%	−4%	−1%	−1%	−1%	−1%

^aAtomic electrostatic charges (ESP). ^bNatural atomic charges.

be seen that, in going from the neutral oxime ether to the radical cation, the positive charge development increases on carbon atoms 2 (14%), 3 (14%), and 5 (17%) as well as on the oxime ether nitrogen atom (10%) (Table 3 and Figure 4). The

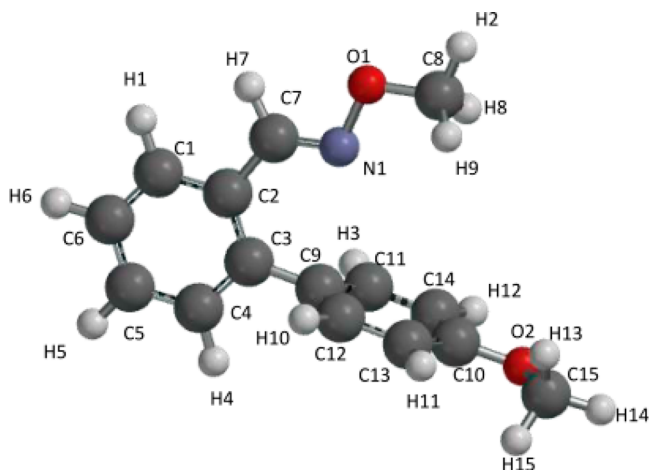
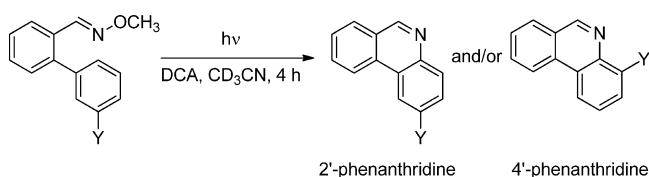


Figure 4. Optimized (AM1) structure of the radical cation of oxime ether **1h** with atom numbers for calculated atomic charge distributions listed in Table 3. Atom numbers for **1i** are identical with the exception of oxygen atom 2.

majority of the positive charge development is found to occur on the benzaldehyde ring and the oxime ether moiety, which is consistent with the observation that the aryl ring acts as a nucleophile and forms the cyclized product in good yield. A similar analysis of compound **1h** shows a different charge distribution upon loss of an electron in the oxime ether. The majority of the positive charge development occurs on carbon atoms 9 (22%) and 10 (16%), as well as oxygen atom 2 (12%). The nitrogen atom of the oxime ether moiety has only 2% of the total charge development. These results clearly show that *para*-substituents such as OCH₃ and OPh attached to the aryl ring cause a shift in the oxidation “location” away from the oxime ether moiety. As a result, nucleophilic attack by the aryl ring onto the nitrogen atom is less likely to happen and the product yield decreases.

The oxidative cyclization pathway of 2'-arylbenzaldehyde *O*-methyl oximes shows an interesting regioselectivity. Biaryl oxime ethers with *meta*-substituted phenyl rings have the ability to cyclize in two different positions, thus creating regioisomers (2'- and 4'-phenanthridines; Scheme 5). In all cases where a reasonable amount of product was formed, the NMR spectra of the photolysis mixtures were very clean and it was possible to determine peak splitting patterns in the crude reaction mixtures. With the exception of compound **1f**, which only showed *E/Z* isomerization, each of the *meta*-compounds

Scheme 5. Potential Regiochemistry in the Formation of Phenanthridines from 2'-Arylbenzaldehyde *O*-Methyl Oxime Ethers



studied (**1b–1e**) favored cyclization to form the corresponding 2'-phenanthridine, as shown by comparison of the reaction products (**2b–2e**) to published NMR spectra of both 2'- and 4'-phenanthridines.²⁴ According to the proposed mechanism, the cyclic carbocation intermediates leading to the two regioisomers have the same degree of stabilization (by resonance), and therefore, we speculate that the observed regiochemistry is due to steric effects in the transition state; the regioisomer that gives the lowest energy conformation to create minimal steric hindrance effects is favored. To test this hypothesis, compound **1m** (3-F) was prepared and studied. The van der Waals radius of fluorine (147 pm) is smaller and closer in size to hydrogen (120 pm) than most other groups or elements,²⁹ and if steric effects are important in this reaction, a smaller substituent would be expected to result in the formation of both regioisomers. Analysis of the NMR spectrum of the cyclic product obtained from the PET reaction of **1m** indicates the presence of both isomers in approximately a 9:1 ratio (2':4'). The fact that a smaller substituent leads to the formation of both isomers (albeit in different amounts) lends some support to the steric argument. It should be noted that the transition-metal-catalyzed cyclization reactions of *O*-acetyl oximes derived from 2'-arylacetophenones studied by Yoshikai did not display this type of regioselectivity when using *meta*-substituted derivatives but rather gave 1:1 mixtures of the two isomers.¹⁰

In addition to the pathways that lead to product formation (phenanthridine, aldehyde, or nitrile), several substrates, including 3- and 4-NO₂ (**1f** and **1k**), showed *E/Z* isomerization as a dominant pathway. The extent of isomerization was determined in the presence and in the absence of the sensitizer. From Table 2, it can be seen that the parent oxime ether (**1a**) shows little isomerization in the absence of DCA at 420 nm (blank). At shorter wavelengths (254, 300, or 350 nm), significant isomerization occurred within 1 h of photolysis. The new isomer did not convert back upon prolonged exposure to light or upon standing for several days. To investigate whether the cyclization was preceded by isomerization, a sample of **1a** was exposed to 300 nm wavelength light for 1 h in the absence of a sensitizer, followed by exposure to 420 nm wavelength light in the presence of DCA for 4 h. When **1a** was photolyzed at 300 nm in the absence of a photosensitizer, the isomer ratio changed from 99:1 to 30:70. Sensitized (DCA) photolysis of this mixture for 4 h at 420 nm gave a 29% yield of **2a**. The isomer ratio after the second photolysis stage was further reduced to 3:97.

Experiments carried out for several of the substituted oxime ethers gave similar results. These results show that photoisomerization is a competing pathway that may prevent the desired oxidative cyclization from taking place. Oxime ethers **1f**, **1g**, and **1k** showed significant isomerization when irradiated in the absence of a photosensitizer. Of these three compounds, only **1g** gave a reasonable amount of the desired cyclized product. Isomerization can also occur at 420 nm wavelength in the presence of DCA, which in some cases is thought to be responsible for the poor cyclization yields. These results suggest that in some cases isomerization leads to an unreactive oxime ether isomer that cannot participate in the desired cyclization reaction.^{30,31}

To determine the synthetic utility of the reaction, several large-scale experiments (10–100 mL) were carried out in order to isolate and quantify the product. The large-scale reaction of **1a** gave an isolated yield of 60% of **2a**, consistent with the yield

determined by ^1H NMR (Table 2). Large-scale reactions of oxime ethers **1d** and **1g** gave yields of 49 and 82% for **2d** and **2g**, respectively, in reasonable agreement with the yields determined by ^1H NMR. The chemical yields for the reactions described here vary from 12 to 94%, and although these numbers leave much to be desired, it is worth pointing out that these reactions are useful for a variety of reasons. Specifically, the synthetic utility of these reactions arises from the fact that under these conditions (a) aldehyde-based oxime ethers do not generate the undesirable nitrile byproducts; (b) the reaction can be accomplished using only a catalytic amount (2 mol %) of the photosensitizer; and (c) the reaction with *meta*-substituents on the aryl ring is regiospecific. None of these characteristics is available in similar reactions currently used to prepare phenanthridines.

In summary, photolysis of 2'-arylbenzaldehyde oxime ethers in the presence of DCA resulted in a regioselective oxidative cyclization reaction. The method uses only a catalytic amount of the photosensitizer, and unlike other similar methods, it did not generate the undesirable nitrile product. A Hammett study showed the involvement of a species with a significant amount of positive charge, and the reaction is proposed to proceed via an oxime ether radical cation intermediate, which undergoes nucleophilic attack by the built-in nucleophile (aromatic ring). A mechanistic analysis revealed a concave downward Hammett plot, which can be explained in terms of a change in the rate-limiting step upon changing the substituents on the 2'-aryl group from electron-withdrawing to electron-donating. Alternatively, computational data suggest that strong electron-donating groups such as OCH_3 and OPh cause a shift in the positive charge distribution away from the oxime ether moiety, decreasing the electrophilic character of the nitrogen atom as well as the nucleophilic character of the aryl ring, leading to a lower yield of the cyclized product. The mechanistic interpretation is consistent with the substituent effect, electrochemical data, and computational ionization potentials. The reaction is regiospecific for *meta*-substituted oxime ethers, favoring cyclization to form only the corresponding 2'-phenanthridine, which is believed to be due to a steric effect. *E/Z* isomerization of the oxime ethers was found in some cases to generate unreactive isomers, limiting the cyclization pathway. Further studies to explore the scope and limitations of systems like these are currently underway.

EXPERIMENTAL SECTION

General Information. All chemicals were obtained from commercial sources and used as supplied without further purification unless otherwise noted. 9,10-Dicyanoanthracene was recrystallized from pyridine at 80 °C. All aqueous bases were prepared by dissolving the appropriate amount of solid by mass into a volumetric flask before being diluted with distilled water and degassed with heat and agitation under vacuum. All GC/MS measurements were performed with a DB-5MS column (30 m \times 0.25 mm \times 0.25 μm) coupled to a quadrupole mass selective detector. Nuclear magnetic resonance spectra were recorded on a 400 MHz instrument and obtained with ^1H decoupling. The data are reported as follows: chemical shift (multiplicity, coupling constant in Hz, integration). Multiplicities are abbreviated as follows: s = singlet, d = doublet, t = triplet, q = quartet, quint = quintet, sept = septet, m = multiplet, and br = broad. All ^1H NMR spectra are reported in δ (ppm) units and are relative to residual solvent signals of CDCl_3 (7.26 ppm) or CD_3CN (1.94 ppm). All ^{13}C NMR spectra are reported in δ (ppm) units and are relative to residual CDCl_3 (77.0 ppm) solvent signals. HRMS measurements were done on one of two different instruments. ESI-MS measurements were carried out using direct infusion electrospray ionization. The samples were dissolved in

methanol and infused directly into the ESI ion source which was interfaced with the time-of-flight mass analyzer in reflectron mode to obtain high-resolution mass measurement. An internal calibrant was used for accurate mass measurement. For GC/MS measurements, the samples were dissolved in dichloromethane (DCM) and injected into the GC column (DB-5) for separation. As the samples elute out of the GC, chemical ionization with ammonia reagent gas was used for generating the ions. These ions were measured with a time-of-flight instrument in reflectron mode for high resolution. During the ionization step, calibrant reagents were added to be used as internal calibrants for the accurate mass measurement.

Oxidation Potentials. Cyclic voltammetry was used to determine oxidation potentials of the oxime ethers dissolved in acetonitrile with tetraethylammonium perchlorate (0.1 M) as the electrolyte. Solutions were degassed under an argon atmosphere and scanned at a rate of 100 mV/s against a Ag/AgCl reference electrode.

General Procedure for Suzuki–Miyaura Cross-Coupling Reactions.^{11,12} An oven-dried 40 mL vial fitted with a screw-top septa was charged with the boronic acid (1 equiv), PdCl_2 (0.05 equiv), PPh_3 (0.15 equiv), and a stirring magnet. The system was evacuated and backfilled with argon three times prior to the addition of DMF (5–10 mL), the aryl bromide (1 equiv), and degassed 2 M Na_2CO_3 (2 equiv) via syringe while stirring. Vials were placed in an oil bath and stirred at 110 °C for >1 h. Reaction progress was monitored by TLC, and the heating ceased once conversion to product had occurred. The mixture was cooled to room temperature before deionized H_2O was added and filtered through Celite, after which it was rinsed with ether. Additional water and diethyl ether were added to separate the aqueous and organic layers. The organic layer was washed with water (3 \times 40 mL), brine (3 \times 40 mL), and 5% LiCl (2 \times 40 mL), while the aqueous layer was washed with diethyl ether (2 \times 40 mL). Solvent was removed by concentrating in vacuo, and the crude product was purified via dry column chromatography (ether/hexane). The purified product was then concentrated by removing solvent in vacuo and dried using a high vacuum equipped with a solvent trap. ^1H NMR spectra were consistent with those reported in literature.^{12,32–39}

Biphenyl-2-carbaldehyde *O*-tert-Butyl Oxime. *N*-tert-Butoxyphthalimide (364.8 mg, 1.6 mmol, 1 equiv) and methylhydrazine (86.2 mg, 1.6 mmol, 1 equiv) reacted in 7 mL DCM for a total of 15 h. Biphenyl-2-carbaldehyde (234.0 mg, 1.6 mmol, 1 equiv) was dissolved in 4 mL ethanol. This solution and glacial acetic acid (101.8 mg, 1.6 mmol, 1 equiv) were added to reaction mixture according to the above *O*-tert-butyl oximation procedure. The reaction was stirred at 70 °C for a total of 24 h to afford the desired product as a light yellow oil (297.9 mg, 92%): ^1H NMR (400 MHz, CDCl_3) δ 1.34 (s, 9 H), 7.29–7.48 (m, 8 H), 8.01–8.08 (m, 1 H), 8.04 (s, 1 H); ^{13}C NMR (101 MHz, CDCl_3) δ 27.6, 79.1, 125.9, 127.3, 127.4, 128.3, 129.0, 129.7, 130.3, 130.7, 139.9, 141.9, 146.2; HRMS (CI) m/z calcd for $\text{C}_{17}\text{H}_{19}\text{NO}$ [$M + 1$] 254.1545, found 254.1540.

4'-Phenoxybiphenyl-2-carbaldehyde. 4-Phenoxyphenylboronic acid (1.2865 g, 6 mmol, 1 equiv), 2-bromobenzaldehyde (700 μL , 6 mmol, 1 equiv), and aqueous 2 M Na_2CO_3 (6 mL, 12 mmol, 2 equiv) reacted in the presence of PdCl_2 (118.4 mg, 0.60 mmol, 0.10 equiv) and PPh_3 (480.6 mg, 1.80 mmol, 0.30 equiv) while dissolved in 30 mL of DMF. The reaction was stirred at 110 °C for 5 min before purification via column chromatography (ether/hexane) to afford the desired product as a white solid (1.5236 g, 93%): mp 69–71 °C; ^1H NMR (400 MHz, CDCl_3) δ 7.07–7.14 (m, 4 H), 7.17 (tt, $J = 7.40$, 1.13 Hz, 1 H), 7.32–7.44 (m, 4 H), 7.44–7.54 (m, 2 H), 7.65 (td, $J = 7.53$, 1.51 Hz, 1 H), 8.03 (ddd, $J = 7.78$, 1.52, 0.75 Hz, 1 H), 10.04 (d, $J = 0.75$ Hz, 1 H); ^{13}C NMR (101 MHz, CDCl_3) δ 118.3, 119.4, 123.9, 127.7, 127.7, 129.9, 130.8, 131.5, 132.4, 133.6, 133.8, 145.3, 156.6, 157.8, 192.4; HRMS (CI) m/z calcd for $\text{C}_{19}\text{H}_{14}\text{O}_2$ [$M + \text{NH}_4$] 292.1338, found 292.1344.

***O*-tert-Butyl Oximation.** A 100 mL round-bottom flask equipped with a stirring magnet was charged with *N*-tert-butoxyphthalimide (1 equiv) and 10 mL of dichloromethane. After dissolution, methylhydrazine (1 equiv) was added and a white precipitate formed. The mixture was stirred at room temperature for >12 h. The aldehyde or ketone (1 equiv) was dissolved in 4 mL of ethanol and was added to

the reaction mixture, followed by the addition of glacial acetic acid (1 equiv). The mixture was stirred and heated to reflux for >12 h. Reaction progress was monitored by TLC, and the heating was ceased once conversion to product occurred. The mixture was cooled to room temperature, and 5 mL of 1 M aq HCl was added. The aqueous layer was extracted with dichloromethane (3 × 20 mL). The combined organic layers were washed with saturated 20 mL aq sodium bicarbonate (NaHCO₃). The aqueous layer was re-extracted with 20 mL of DCM. Organic extracts were dried using anhydrous sodium sulfate (Na₂SO₄), and solvent was removed by concentrating in vacuo. The crude product was dried using a high vacuum equipped with a solvent trap. In some cases, products were purified by dry column chromatography (EtOAc/hexane eluent). Products were characterized by gas chromatography mass spectrometry (GC-MS) and nuclear magnetic resonance spectroscopy (¹H NMR and ¹³C NMR).

1-([1,1'-Biphenyl]-2-yl)ethanone *O*-tert-Butyl Oxime. *N*-tert-Butoxyphthalimide (453.7 mg, 2 mmol, 1 equiv) and methylhydrazine (182.2 mg, 2 mmol, 1 equiv) reacted in 5 mL of DCM for a total of 15 h. 1-([1,1'-Biphenyl]-2-yl)ethanone (406.8 mg, 2 mmol, 1 equiv) was dissolved in 4 mL of ethanol. This solution and glacial acetic acid (131.3 mg, 2 mmol, 1 equiv) were added to reaction mixture according to the above *O*-tert-butyl oximation procedure. The reaction was stirred at 70 °C for a total of 24 h to afford the desired product as a clear oil (495.9 mg, 92%): ¹H NMR (400 MHz, CDCl₃) δ 1.30 (s, 9 H), 1.70 (s, 3 H), 7.29–7.48 (m, 9 H); ¹³C NMR (101 MHz, CDCl₃) δ ppm 16.4, 27.7, 78.1, 127.0, 127.2, 128.2, 128.4, 129.0, 129.3, 130.2, 138.0, 140.5, 141.5, 156.0; HRMS (CI) *m/z* calcd for C₁₈H₂₁NO [M + Na] 290.1521, found 290.1528.

***O*-Methyl Oximation.** A 40 mL vial fitted with a screw-top septa and equipped with a stirring magnet was charged with the aldehyde (1 equiv), methoxylamine hydrochloride (CH₃ONH₂·HCl, 98%, 2 equiv), and solid sodium acetate (NaOAc, 4.5 equiv) or sodium hydroxide (NaOH, 4.5 equiv) before dissolution in 20 mL of 50% ethanol in water. The mixture was stirred and heated at 85 °C. Reaction progress was monitored by TLC, and the heating was ceased once conversion to product occurred. The mixture was cooled to room temperature and extracted with dichloromethane (3 × 20 mL). Solvent was removed by concentrating in vacuo, and the crude product was dried using a high vacuum equipped with a solvent trap. In some cases, products were purified by dry column chromatography (ether/hexane). Products were characterized by GC-MS and nuclear magnetic resonance spectroscopy (¹H NMR and ¹³C NMR).

Biphenyl-2-carbaldehyde *O*-Methyl Oxime (1a). Biphenyl-2-carbaldehyde (352.3 mg, 1.9 mmol, 1 equiv) and methoxylamine hydrochloride (579.3 mg, 6.9 mmol, 3.5 equiv) reacted in the presence of NaOH (9 mmol, 4.5 equiv) while dissolved in 13 mL of 38% ethanol in water. The reaction was stirred at 85 °C for a total of 1.5 h to afford the desired product as a light yellow oil (404.3 mg, 99%): ¹H NMR (400 MHz, CDCl₃) δ 3.96 (s, 3 H), 7.29–7.47 (m, 8 H), 7.98 (dd, *J* = 7.53, 1.51 Hz, 1 H), 8.05 (s, 1 H); ¹³C NMR (101 MHz, CDCl₃) δ 61.9, 126.0, 127.5, 127.5, 128.3, 129.5, 129.7, 129.7, 130.2, 139.5, 142.1, 147.9; HRMS (CI) *m/z* calcd for C₁₄H₁₃NO [M + Na] 234.0895, found 234.0903.

3'-Chlorobiphenyl-2-carbaldehyde *O*-Methyl Oxime (1b). 3'-Chlorobiphenyl-2-carbaldehyde (147.8 mg, 0.66 mmol, 1 equiv) and methoxylamine hydrochloride (110.2 mg, 1.31 mmol, 2 equiv) reacted in the presence of NaOAc (241.7 mg, 2.95 mmol, 4.5 equiv) while dissolved in 20 mL of 50% ethanol in water. The reaction was stirred at 85 °C for a total of 1 h to afford the desired product as a light yellow oil (137.2 mg, 82%): ¹H NMR (400 MHz, CDCl₃) δ 3.95 (s, 3 H), 7.16–7.20 (m, 1 H), 7.27–7.46 (m, 6 H), 7.95–7.98 (m, 1 H), 7.98 (s, 2 H), 7.99 (s, 1 H); ¹³C NMR (101 MHz, CDCl₃) δ 62.0, 126.2, 127.7, 128.0, 128.1, 129.5, 129.6, 129.6, 129.7, 130.1, 134.3, 140.5, 141.4, 147.2; HRMS (CI) *m/z* calcd for C₁₄H₁₂ClNO [M + Na] 268.0505, found 268.0499.

3'-Methoxybiphenyl-2-carbaldehyde *O*-Methyl Oxime (1c). 3'-Methoxybiphenyl-2-carbaldehyde (139.3 mg, 0.66 mmol, 1 equiv) and methoxylamine hydrochloride (112.2 mg, 1.3 mmol, 2 equiv) reacted in the presence of NaOAc (252.4 mg, 3.1 mmol, 4.5 equiv) while dissolved in 20 mL of 50% ethanol in water. The reaction was stirred

at 85 °C for a total of 1 h to afford the desired product as a white solid (145.0 mg, 92%): mp 58–59 °C; ¹H NMR (400 MHz, CDCl₃) δ 3.84 (s, 3 H), 3.96 (s, 3 H), 6.83–6.98 (m, 3 H), 7.31–7.46 (m, 4 H), 7.97 (dd, *J* = 7.78, 1.51 Hz, 1 H), 8.06 (s, 1 H); ¹³C NMR (101 MHz, CDCl₃) δ 55.2, 61.9, 113.0, 115.3, 122.2, 125.9, 127.6, 129.3, 129.5, 129.7, 130.0, 140.9, 141.9, 147.8, 159.4; HRMS (CI) *m/z* calcd for C₁₅H₁₅NO₂ [M + Na] 264.1000, found 264.0998.

3'-Methylbiphenyl-2-carbaldehyde *O*-Methyl Oxime (1d). 3'-Methylbiphenyl-2-carbaldehyde (390.4 mg, 2 mmol, 1 equiv) and methoxylamine hydrochloride (334.1 mg, 4 mmol, 2 equiv) reacted in the presence of NaOAc (736.4 mg, 9 mmol, 4.5 equiv) while dissolved in 40 mL of 50% ethanol in water. The reaction was stirred at 85 °C for a total of 1 h to afford the desired product as a light yellow oil (291.2 mg, 65%): ¹H NMR (400 MHz, CDCl₃) δ 2.04 (s, 3 H), 3.90 (s, 3 H), 7.10 (dd, *J* = 7.28, 1.00 Hz, 1 H), 7.14–7.31 (m, 4 H), 7.32–7.43 (m, 2 H), 7.73 (s, 6 H), 7.96–8.01 (m, 1 H); ¹³C NMR (101 MHz, CDCl₃) δ 21.4, 61.9, 125.9, 126.8, 127.4, 128.1, 128.2, 129.4, 129.6, 130.2, 130.3, 137.9, 139.5, 142.3, 147.9; HRMS (CI) *m/z* calcd for C₁₅H₁₅NO [M + Na] 248.1051, found 248.1049.

3'-(Trifluoromethyl)biphenyl-2-carbaldehyde *O*-Methyl Oxime (1e). 3'-(Trifluoromethyl)biphenyl-2-carbaldehyde (427.4 mg, 1.71 mmol, 1 equiv) and methoxylamine hydrochloride (288.3 mg, 3.42 mmol, 2 equiv) reacted in the presence of NaOAc (631.4 mg, 7.7 mmol, 4.5 equiv) while dissolved in 20 mL of 50% ethanol in water. The reaction was stirred at 85 °C for a total of 7 h to afford the desired product as a light yellow oil (305.5 mg, 64%): ¹H NMR (400 MHz, CDCl₃) δ 3.96 (s, 3 H), 7.29–7.35 (m, 1 H), 7.40–7.49 (m, 4 H), 7.70 (d, *J* = 8.28 Hz, 2 H), 7.97 (s, 1 H), 7.99 (dd, *J* = 6.78, 1.25 Hz, 1 H); ¹³C NMR (101 MHz, CDCl₃) δ 61.9, 124.0 (q, ¹*J*_{CF} = 272 Hz), 124.3 (q, ³*J*_{CF} = 3.67 Hz), 125.4, 126.2 (q, ³*J*_{CF} = 3.67 Hz), 126.4, 128.2, 128.7, 129.7, 129.8, 130.1, 130.9 (q, ²*J*_{CF} = 32.28 Hz), 133.1 (q, ⁵*J*_{CF} = 1.47 Hz), 140.4 (m), 147.0; HRMS (CI) *m/z* calcd for C₁₅H₁₂F₃NO [M + 1] 280.0949, found 280.0957.

3'-Nitrobiphenyl-2-carbaldehyde *O*-Methyl Oxime (1f). 3'-Nitrobiphenyl-2-carbaldehyde (681.0 mg, 3 mmol, 1 equiv) and methoxylamine hydrochloride (501.1 mg, 6 mmol, 2 equiv) reacted in the presence of NaOAc (1.1074 g, 13.5 mmol, 4.5 equiv) while dissolved in 40 mL of 50% ethanol in water. The reaction was stirred at 85 °C for a total of 20 h to afford the desired product as a tan solid (406.3 mg, 53%): mp 114–116 °C; ¹H NMR (400 MHz, CDCl₃) δ 3.96 (s, 3 H), 7.31–7.35 (m, 1 H), 7.42–7.52 (m, 2 H), 7.59–7.68 (m, 2 H), 7.95 (s, 1 H), 7.97–8.03 (m, 1 H), 8.22 (dt, *J* = 1.69, 1.04 Hz, 1 H), 8.26 (dt, *J* = 7.28, 2.13 Hz, 1 H); ¹³C NMR (101 MHz, CDCl₃) δ 62.0, 122.3, 124.2, 126.5, 128.6, 129.2, 129.7, 129.8, 130.0, 135.6, 139.1, 141.2, 146.5, 148.1; HRMS (CI) *m/z* calcd for C₁₄H₁₂N₂O₃ [M + Na] 279.0746, found 279.0742.

4'-Chlorobiphenyl-2-carbaldehyde *O*-Methyl Oxime (1g). 4'-Chlorobiphenyl-2-carbaldehyde (145.1 mg, 0.66 mmol, 1 equiv) and methoxylamine hydrochloride (111.0 mg, 1.31 mmol, 2 equiv) reacted in the presence of NaOAc (241.8 mg, 2.95 mmol, 4.5 equiv) while dissolved in 20 mL of 50% ethanol in water. The reaction was stirred at 85 °C for a total of 1 h to afford the desired product as a yellow oil (128.9 mg, 78%): ¹H NMR (400 MHz, CDCl₃) δ 3.94 (s, 3 H), 7.21–7.25 (m, 2 H), 7.26–7.30 (m, 1 H), 7.31–7.43 (m, 5 H), 7.94–7.97 (m, 1 H), 7.98 (s, 1 H); ¹³C NMR (101 MHz, CDCl₃) δ 62.0, 126.2, 127.9, 128.5, 129.6, 129.7, 130.0, 131.0, 133.7, 138.0, 140.7, 147.4; HRMS (CI) *m/z* calcd for C₁₄H₁₂ClNO [M + H] 246.0686, found 246.0686.

4'-Methoxybiphenyl-2-carbaldehyde *O*-Methyl Oxime (1h). 4'-Methoxybiphenyl-2-carbaldehyde (128.3 mg, 0.6 mmol, 1 equiv) and methoxylamine hydrochloride (104.3 mg, 1.2 mmol, 2 equiv) reacted in the presence of NaOAc (224.9 mg, 2.7 mmol, 4.5 equiv) while dissolved in 20 mL of 50% ethanol in water. The reaction was stirred at 85 °C for a total of 2 h to afford the desired product as a white solid (144.3 mg, 99%): mp 49–51 °C; ¹H NMR (400 MHz, CDCl₃) δ 3.87 (s, 3 H), 3.96 (s, 3 H), 6.95–7.00 (m, 2 H), 7.22–7.27 (m, 2 H), 7.30–7.38 (m, 2 H), 7.39–7.45 (m, *J* = 1.51 Hz, 1 H), 7.95 (dd, *J* = 7.78, 1.51 Hz, 1 H), 8.06 (s, 1 H); ¹³C NMR (101 MHz, CDCl₃) δ 55.3, 61.9, 113.8, 126.1, 127.2, 129.5, 129.7, 130.2, 130.8, 131.9, 141.8,

148.1, 159.1; HRMS (CI) m/z calcd for $C_{15}H_{15}NO_2$ [$M + Na$] 264.1000, found 264.1003.

4'-Methylbiphenyl-2-carbaldehyde O-Methyl Oxime (1i). 4'-Methylbiphenyl-2-carbaldehyde (551.8 mg, 2.8 mmol, 1 equiv) and methoxylamine hydrochloride (460.8 mg, 5.6 mmol, 2 equiv) reacted in the presence of NaOAc (1.0411 g, 12.6 mmol, 4.5 equiv) while dissolved in 40 mL of 50% ethanol in water. The reaction was stirred at 85 °C for a total of 46 h to afford the desired product as a dark orange oil (440.7 mg, 70%): 1H NMR (400 MHz, $CDCl_3$) δ 2.41 (s, 3 H), 3.96 (s, 3 H), 7.19–7.26 (m, 2 H), 7.23 (d, $J = 7.53$ Hz, 2 H), 7.30–7.47 (m, 4 H), 7.94–7.98 (m, 1 H), 8.06 (s, 1 H); ^{13}C NMR (101 MHz, $CDCl_3$) δ 21.1, 61.9, 126.0, 127.3, 129.0, 129.5, 129.6, 129.7, 130.2, 136.6, 137.2, 142.1, 148.0; HRMS (CI) m/z calcd for $C_{15}H_{15}NO$ [$M + H$] 226.1232, found 226.1231.

4'-(Trifluoromethyl)biphenyl-2-carbaldehyde O-Methyl Oxime (1j). 4'-(Trifluoromethyl)biphenyl-2-carbaldehyde (957.0 mg, 3.83 mmol, 1 equiv) and methoxylamine hydrochloride (646.1 mg, 7.67 mmol, 2 equiv) reacted in the presence of NaOAc (1.4138 g, 17.235 mmol, 4.5 equiv) while dissolved in 40 mL of 50% ethanol in water. The reaction was stirred at 85 °C for a total of 1 h to afford the desired product as a tan solid (808.0 mg, 76%): mp 66–68 °C; 1H NMR (400 MHz, $CDCl_3$) δ 3.96 (s, 3 H), 7.30–7.35 (m, 1 H), 7.40–7.52 (m, 3 H), 7.56 (t, $J = 7.53$ Hz, 1 H), 7.60 (s, 1 H), 7.63–7.69 (m, 1 H), 7.97 (s, 1 H), 8.00 (dd, $J = 7.53$, 1.76 Hz, 1 H); ^{13}C NMR (101 MHz, $CDCl_3$) δ 61.9, 124.1 (q, $^1J_{CF} = 272$ Hz), 125.3 (q, $^3J_{CF} = 3.67$ Hz), 126.3, 128.3, 129.7, 129.7 (q, $^2J_{CF} = 33$ Hz), 129.8, 130.0, 143.2 (q, $^5J_{CF} = 1.47$ Hz), 147.0; HRMS (CI) m/z calcd for $C_{15}H_{12}F_3NO$ [$M + 1$] 280.0949, found 280.0960.

4'-Nitrobiphenyl-2-carbaldehyde O-Methyl Oxime (1k). 4'-Nitrobiphenyl-2-carbaldehyde (733.5 mg, 3.23 mmol, 1 equiv) and methoxylamine hydrochloride (547.0 mg, 6.46 mmol, 2 equiv) reacted in the presence of NaOAc (1.1945 g, 14.54 mmol, 4.5 equiv) while dissolved in 32 mL of 50% ethanol in water. The reaction was stirred at 85 °C for a total of 2.5 h to afford the desired product as a tan solid (437.3 mg, 53%): mp 113–116 °C; 1H NMR (400 MHz, $CDCl_3$) δ 3.96 (s, 3 H), 7.31–7.35 (m, 1 H), 7.45–7.53 (m, 4 H), 7.95 (s, 1 H), 7.98–8.02 (m, 1 H), 8.28–8.34 (m, 2 H); ^{13}C NMR (101 MHz, $CDCl_3$) δ 61.9, 123.4, 126.5, 128.6, 129.6, 129.7, 129.7, 130.1, 130.4, 139.3, 144.5, 146.2, 146.4, 147.1; HRMS (CI) m/z calcd for $C_{14}H_{12}N_2O_3$ [$M + H$] 257.0926, found 257.0922.

4'-Phenoxybiphenyl-2-carbaldehyde O-Methyl Oxime (1l). 4'-Phenoxybiphenyl-2-carbaldehyde (190.2 mg, 0.66 mmol, 1 equiv) and methoxylamine hydrochloride (111.8 mg, 1.31 mmol, 2 equiv) reacted in the presence of NaOAc (279.7 mg, 2.95 mmol, 4.5 equiv) while dissolved in 20 mL of 50% ethanol in water. The reaction was stirred at 85 °C for a total of 1 h to afford the desired product as a white solid (200.8 mg, 95%): mp 67–68 °C; 1H NMR (400 MHz, $CDCl_3$) δ 3.95 (s, 3 H), 7.02–7.06 (m, $J = 8.78$ Hz, 2 H), 7.06–7.10 (m, 2 H), 7.14 (tt, $J = 7.40$, 1.13 Hz, 1 H), 7.23–7.28 (m, $J = 8.78$ Hz, 2 H), 7.29–7.45 (m, 5 H), 7.95 (dd, $J = 7.53$, 1.51 Hz, 1 H), 8.07 (s, 1 H); ^{13}C NMR (101 MHz, $CDCl_3$) δ 61.9, 118.3, 119.4, 123.6, 126.2, 127.5, 129.6, 129.7, 129.8, 130.2, 131.0, 134.3, 141.4, 147.8, 156.8, 157.1; HRMS (CI) m/z calcd for $C_{20}H_{17}NO_2$ [$M + H$] 304.1338, found 304.1330.

3'-Fluorobiphenyl-2-carbaldehyde O-Methyl Oxime (1m). 2'-Fluorobiphenyl-2-carbaldehyde (169.5 mg, 0.85 mmol, 1 equiv) and methoxylamine hydrochloride (142.6 mg, 1.7 mmol, 2 equiv) reacted in the presence of NaOAc (319.9 mg, 3.83 mmol, 4.5 equiv) while dissolved in 20 mL of 50% ethanol in water. The reaction was stirred at 85 °C for a total of 1.5 h to afford the desired product as a light yellow oil (196.5 mg, 99%): 1H NMR (400 MHz, $CDCl_3$) δ 3.97 (s, 3 H), 7.01–7.12 (m, 3 H), 7.29–7.34 (m, 1 H), 7.35–7.48 (m, 3 H), 7.95–8.01 (m, 1 H), 8.02 (s, 1 H); ^{13}C NMR (101 MHz, $CDCl_3$) δ 62.0, 114.4 (d, $^2J_{CF} = 20.54$ Hz), 116.6 (d, $^2J_{CF} = 21.27$ Hz), 125.5 (d, $^4J_{CF} = 2.93$ Hz), 126.2, 128.0, 129.6, 129.7 (d, $^3J_{CF} = 6.60$ Hz), 129.9, 130.0, 140.7 (d, $^4J_{CF} = 2.20$ Hz), 141.8 (d, $^3J_{CF} = 7.34$ Hz), 147.4, 162.6 (d, $^1J_{CF} = 247$ Hz); HRMS (CI) m/z calcd for $C_{14}H_{12}FNO$ [$M + H$] 230.0981, found 230.0970.

Photolysis of Oxime Ethers. Three nuclear magnetic resonance (NMR) tubes were each charged with DCA (0.015–5 μ mol, 0.001–

0.33 equiv), the oxime ether (15 μ mol, 1 equiv), and 1 mL of acetonitrile- d_3 (CD_3CN) or benzene- d_6 (C_6D_6). The samples were photolyzed at 420 nm using a photoreactor equipped with nine mercury vapor lamps for a total of 4 h, unless otherwise noted. An internal standard of either 4-nitrobenzylbromide or 4-nitrobenzaldehyde was added following photolysis to determine product yield by 1H NMR. GC-MS was also used to verify product formation. Whenever available, the product NMR spectra were compared to those available in the literature: **2a**,³⁹ **2b**,²⁵ **2c**,²⁵ **2d**,⁴⁰ **2e**,²⁶ **2f**,²⁷ **2g**,²⁵ **2h**,^{41,42} **2i**,²⁶ **2j**,⁴² and **2m**.^{42,43}

■ ASSOCIATED CONTENT

● Supporting Information

NMR spectra for new compounds; descriptions and results from photolysis experiments; and tabulated data for calculated charge distributions. This material is available free of charge via the Internet at <http://pubs.acs.org>.

■ AUTHOR INFORMATION

Corresponding Author

*E-mail: pdelijser@fullerton.edu.

Notes

The authors declare no competing financial interest.

■ ACKNOWLEDGMENTS

This material is based upon work supported by the National Science Foundation under Grant No. CHE-0844110.

■ REFERENCES

- (1) (a) Beckmann, E. *Ber. Bunsen-Ges. Phys. Chem.* **1886**, *19*, 988. (b) Gawley, R. E. *Org. React.* **1988**, *35*, 14–24. (c) Gregory, B. J.; Moodie, R. B.; Schofield, K. *J. Chem. Soc. (B)* **1970**, 338.
- (2) (a) Bieleman, J. H.; Bolle, T.; Braig, A.; Glaser, J. K.; Spang, R.; Köhler, M.; Valet, A. In *Additives for Coatings*; Bieleman, J. H., Ed.; Wiley-VCH: Weinheim, Germany, 2000; pp 257–348. (b) van Gorkum, R.; Bouwman, E. *Coord. Chem. Rev.* **2005**, *249*, 1709.
- (3) Tanase, S.; Hierso, J.-C.; Bouwman, E.; Reedijk, J.; ter Borg, J.; Bieleman, J. H.; Schut, A. *New J. Chem.* **2003**, *27*, 854.
- (4) de Lijser, H. J. P.; Fardoun, F. H.; Sawyer, J. R.; Quant, M. *Org. Lett.* **2002**, *4*, 2325.
- (5) (a) de Lijser, H. J. P.; Kim, J. S.; McGorty, S. M.; Ulloa, E. M. *Can. J. Chem.* **2003**, *81*, 575. (b) Park, A.; Kosareff, N. M.; Kim, J. S.; de Lijser, H. J. P. *Photochem. Photobiol.* **2006**, *82*, 110.
- (6) de Lijser, H. J. P.; Hsu, S.; Marquez, B. V.; Park, A.; Sanguantrakun, N.; Sawyer, J. R. *J. Org. Chem.* **2006**, *71*, 7785.
- (7) de Lijser, H. J. P.; Burke, C. R.; Rosenberg, J.; Hunter, J. J. *Org. Chem.* **2009**, *74*, 1679.
- (8) de Lijser, H. J. P.; Tsai, C. K. *J. Org. Chem.* **2004**, *69*, 3057.
- (9) de Lijser, H. J. P.; Rangel, N. A.; Tetelman, M. A.; Tsai, C. K. *J. Org. Chem.* **2007**, *72*, 4126.
- (10) Deb, I.; Yoshikai, N. *Org. Lett.* **2013**, *15*, 4254 and references therein.
- (11) Miyaura, N.; Yamada, K.; Suzuki, A. *Tetrahedron Lett.* **1979**, *20*, 3437.
- (12) Ye, F.; Shi, Y.; Zhou, L.; Xiao, Q.; Zhang, Y.; Wang, J. *Org. Lett.* **2011**, *13*, 5020.
- (13) (a) Rhodes, C. J. *J. Chem. Soc., Faraday Trans.* **1990**, *86*, 3303. (b) Bordwell, F. G.; Guo, Z. J. *J. Org. Chem.* **1992**, *57*, 3019.
- (14) (a) Alonso, R.; Campos, P. J.; García, B.; Rodríguez, M. A. *Org. Lett.* **2006**, *8*, 3521. (b) Alonso, R.; Caballero, A.; Campos, P. J.; Rodríguez, M. A. *Tetrahedron* **2010**, *66*, 8828.
- (15) McBurney, R. T.; Slawin, A. M. Z.; Smart, L. A.; Yu, Y.; Walton, J. C. *Chem. Commun.* **2011**, *47*, 7974.
- (16) Several *ortho*-substituted 2'-arylbenzaldehyde oxime ethers were prepared and studied, as well; however, they did not produce the desired phenanthridine products in good yields. Instead, in some cases,

significant amounts of **2a** were formed, suggesting an *ipso*-substitution reaction. This pathway is currently being investigated.

(17) Rehm, D.; Weller, A. *Isr. J. Chem.* **1970**, *8*, 259.

(18) Gould, I. R.; Ege, D.; Moser, J. E.; Faird, S. *J. Am. Chem. Soc.* **1990**, *112*, 4290.

(19) Brown, H. C.; Okamoto, Y. *J. Am. Chem. Soc.* **1958**, *80*, 4979.

(20) (a) Leffler, J. E.; Grunwald, E. *Rates and Equilibria of Organic Reactions*; John Wiley and Sons, Inc.: New York, 1963; p 189.

(b) Hart, H.; Sedor, E. A. *J. Am. Chem. Soc.* **1967**, *89*, 2342.

(21) Ionization potentials were calculated at the AM1²² level of theory using Spartan: Spartan '08, Wave function, Inc., 18401 Von Karman Avenue, Suite 370, Irvine, CA 92715 USA.

(22) AM1 calculations: Dewar, M. J. S.; Zoebisch, E. G.; Healy, E. F.; Stewart, J. J. P. *J. Am. Chem. Soc.* **1985**, *107*, 3902.

(23) (a) Lorrance, E. D.; Kramer, W. H.; Gould, I. R. *J. Am. Chem. Soc.* **2002**, *124*, 15225. (b) Lorrance, E. D.; Kramer, W. H.; Gould, I. R. *J. Am. Chem. Soc.* **2004**, *126*, 14071.

(24) Comparison of the reaction products (**2b–2e**) to published NMR spectra of both 2'- and 4'-phenanthridines reveals similarities only with 2'-phenanthridine isomers.^{25–28} For example, the ¹H NMR spectrum for *meta*-Cl-substituted phenanthridine (**2b**) contains a doublet at 8.75 ppm with a ⁴J = 2.3 Hz, indicating that this singlet was split by a *meta*-proton. A doublet of doublets at 7.78 ppm contains coupling constants of ³J = 8.6 Hz and ⁴J = 2.3 Hz, suggesting that this proton is adjacent to the C–Cl group and was split not only by its *ortho*-proton but also by the *meta*-proton at 8.75 ppm. Other doublets at 8.72, 8.20, and 8.15 ppm all displayed ³J values of 6.4, 7.9, and 8.8 Hz, respectively. The two triplets at 7.99 and 7.86 ppm also displayed both ³J and ⁴J coupling (Figure S1).

(25) Budén, M. E.; Dorn, V. B.; Gamba, M.; Pierini, A. B.; Rossi, R. *A. J. Org. Chem.* **2010**, *75*, 2206.

(26) Intrieri, D.; Mariani, M.; Caselli, A.; Ragaini, F.; Gallo, E. *Chem.—Eur. J.* **2012**, *18*, 10487.

(27) Linsenmeier, A. M.; Williams, C. M.; Bräse, S. *J. Org. Chem.* **2011**, *76*, 9127.

(28) Maestri, G.; Larraufie, M. H.; Derat, E.; Ollivier, C.; Fensterbank, L.; Lacôte, E.; Malacria, M. *Org. Lett.* **2010**, *12*, 5692.

(29) Bondi, A. *J. Phys. Chem.* **1964**, *68*, 441.

(30) It has been reported that the photosensitized isomerization of the carbon–nitrogen double bond may be an oxygen-sensitive process.³¹ To determine whether the presence of oxygen negatively affected the desired oxidative cyclization pathway (by promoting the isomerization pathway), experiments were also carried out in the absence of oxygen. An argon-purged solution of the 3-NO₂ (**1f**) derivative was found to give the same yield of the phenanthridine product **2f** upon photolysis in the presence of DCA as the air-saturated solution. The amount of isomerization was found to be slightly greater in the absence of air (60:40 instead of 70:30).

(31) Kawamura, Y.; Takayama, R.; Nishiuchi, M.; Tsukayama, M. *Tetrahedron Lett.* **2000**, *41*, 8101.

(32) Chosson, E.; Rochais, C.; Legay, R.; Sopkova de Oliveira Santos, J.; Rault, S.; Dallemagne, P. *Tetrahedron* **2011**, *67*, 2548.

(33) Iuliano, A.; Piccioli, P.; Fabbri, D. *Org. Lett.* **2004**, *6*, 3711.

(34) Motti, E.; Della Ca', N.; Xu, D.; Piersimoni, A.; Bedogni, E.; Zhou, Z.-M.; Catellani, M. *Org. Lett.* **2012**, *14*, 5792.

(35) Chamoin, S.; Houldsworth, S.; Kruse, C. G.; Iwema Bakker, W.; Snieckus, V. *Tetrahedron Lett.* **1998**, *39*, 4179.

(36) Dupuis, C.; Adiey, K.; Charruault, L.; Michelet, V.; Savignac, M.; Genêt, J.-P. *Tetrahedron Lett.* **2001**, *42*, 6523.

(37) Zhao, J.; Yue, D.; Campo, M. A.; Larock, R. C. *J. Am. Chem. Soc.* **2007**, *129*, 5288.

(38) Sindelar, M.; Lutz, T. A.; Petrera, M.; Wanner, K. T. *J. Med. Chem.* **2013**, *56*, 1323.

(39) Read, M. L.; Gundersen, L.-L. *J. Org. Chem.* **2013**, *78*, 1311.

(40) Li, Z.; Fan, F.; Yang, J.; Liu, Z.-Q. *Org. Lett.* **2014**, *16*, 3396.

(41) Li, D.; Zhao, B.; LaVoie, E. J. *J. Org. Chem.* **2000**, *65*, 2802.

(42) Portela-Cubillo, F.; Scott, J. S.; Walton, J. C. *J. Org. Chem.* **2008**, *73*, 5558.

(43) Liu, Y.-Y.; Song, R.-J.; Wu, C.-Y.; Gong, L.-B.; Hu, M.; Wang, Z.-Q.; Xie, Y.-X.; Li, J.-H. *Adv. Synth. Catal.* **2012**, *354*, 347.